

# Tetrahydrofuran Activates Fluorescence Resonant Energy Transfer from a Cationic Conjugated Polyelectrolyte to Fluorescein-Labeled DNA in Aqueous Media

Bin Liu\*<sup>[a]</sup> and Guillermo C. Bazan\*<sup>[b]</sup>

**Abstract:** A cationic water-soluble conjugated polyelectrolyte, poly[9,9-bis(6''-(*N,N,N*-trimethylammonium)hexyl)-fluorene-*co-alt*-2,5-bis(6'-(*N,N,N*-trimethylammonium)hexyloxyphenylene) tetrabromide], was synthesized. Fluorescence resonant energy transfer (FRET) experiments between the polymer and fluorescein-labeled single-stranded DNA (ssDNA-FI) were conducted in aqueous buffer and THF/buffer mixtures. Weak fluorescence emission in aqueous buffer was observed upon excitation of the polymer,

whereas addition of THF turned on the fluorescence. Fluorescence self-quenching of ssDNA-FI in the ssDNA-FI/polymer complexes as well as electron transfer from the polymer to fluorescein may account for the low fluorescence emission in buffer. The improved sensitization of fluorescence by the po-

**Keywords:** chromophores • DNA • electron transfer • fluorescence • FRET (fluorescence resonant energy transfer)

lymer observed in THF/buffer could be attributed to the weaker binding between the polymer and ssDNA-FI and a decrease in dielectric constant of the solvent mixture, which disfavors electron transfer. THF-assisted signal sensitization was also observed for the polymer and fluorescein-labeled double-stranded DNA (dsDNA-FI). These results indicate that the use of cosolvent provides a strategy to improve the detection sensitivity for biosensors based on the optical amplification provided by conjugated polymers.

## Introduction

Water-soluble conjugated polyelectrolytes (CPs) form the basis of highly sensitive DNA sensors.<sup>[1]</sup> Recently, we reported fluorescence turn-on assays based on cationic CPs (CCPs) and fluorescence resonant energy transfer (FRET) from CPs to chromophore (C\*)-labeled probes for strand-specific detection of DNA and RNA in aqueous media.<sup>[2]</sup> Amplification of C\* emission by excitation of CCPs, relative

to direct excitation of C\*, originates from the light-harvesting properties of the polymer.<sup>[1b]</sup>

Efficient CCP→C\* FRET is a required condition for the increase of sensitivity.<sup>[3]</sup> Maximized spectral overlap between the emission of the CCP and the absorption of C\*, improved registry between transition moments, and shortened distances between CCP and the signaling C\* should provide for better FRET conditions.<sup>[4]</sup> A recent report showed that improved energy-transfer efficiencies could be achieved by using shape-adaptable polymers, which have more conformational freedom and improved registry with analyte shape, as compared to their linear counterparts.<sup>[2f]</sup> Efforts have also been made to tune the conjugated polymer emission to match different probe chromophores.<sup>[2c]</sup>

Recent studies involving cationic poly(fluorene-cophenylene) derivatives and single-stranded DNA (ssDNA) labeled with chromophores of different orbital energy levels highlight the importance of properly matching the donor and acceptor energy levels to favor FRET.<sup>[5]</sup> Competition between FRET and electron-transfer events as a function of the HOMO and LUMO energies in donor/acceptor pairs has also been reported for conjugated phenylenevinylene-based dendrimers, in which acceptor emission is strongly influenced by the solvent.<sup>[6]</sup>

[a] Prof. B. Liu

Department of Chemical and Biomolecular Engineering  
National University of Singapore  
4 Engineering Drive 4, Singapore 117576 (Singapore)  
Fax: (+65) 6779-1936  
E-mail: cheliub@nus.edu.sg

[b] Prof. G. C. Bazan

Department of Materials and Chemistry & Biochemistry  
Institute for Polymers and Organic Solids  
University of California at Santa Barbara, CA 93106 (USA)  
Fax: (+1) 805-893-4120  
E-mail: bazan@chem.ucsb.edu

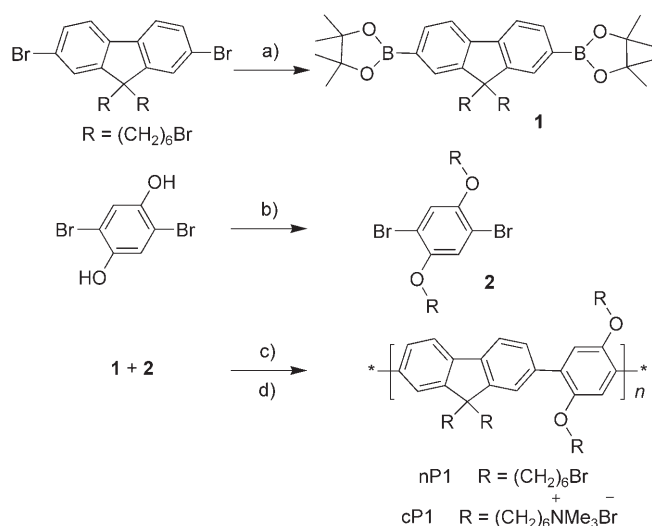


Supporting information for this article is available on the WWW under <http://www.chemasianj.org> or from the author.

Herein, we report the synthesis and characterization of water-soluble poly[9,9-bis(6''-(*N,N,N*-trimethylammonium)-hexylfluorene-*co-alt*-2,5-bis(6'-(*N,N,N*-trimethylammonium)-hexyloxyphenylene) tetrabromide] (cP1) and an FRET study with fluorescein (Fl)-labeled single-stranded DNA (ssDNA-Fl). Fl was chosen as the acceptor because of the spectral overlap between cP1 emission and Fl absorption, which meets FRET requirements. Additionally, the orbital energy levels of cP1 and Fl are arranged so that photoinduced electron transfer is a viable process.<sup>[5]</sup> We show higher Fl emission and weaker binding strength of the interpolyelectrolyte complexes in the presence of THF, which leads to an increase in FRET efficiency, at the expense of the electron-transfer process. Similar observations were obtained with cP1 and Fl-labeled double-stranded DNA (dsDNA-Fl). These results indicate that the use of cosolvent may serve to improve the detection sensitivity for conjugated polymer-based biosensors and to obtain an insight into the energetics of the photophysical processes in these self-assembled systems.

## Results and Discussion

As shown in Scheme 1, the synthesis of cP1 involved palladium-mediated Suzuki cross-coupling copolymerization of bis[9,9'-bis(6''-bromohexyl)fluorenyl]-4,4,5,5-tetramethyl[1.3.2]-dioxaborolane and 1,4-dibromo-2,5-bis(6-bromohexyloxy)benzene to afford the neutral precursor polymer nP1. Subsequent quaternization yielded the target structure. The key intermediate in the polymerization, 2,7-bis[9,9'-bis(6''-bromohexyl)fluorenyl]-4,4,5,5-tetramethyl[1.3.2]dioxaborolane, was synthesized through a simplified new method by heating a mixture of 2,7-dibromo-9,9'-bis(6''-bromohexyl)fluorene



Scheme 1. Synthesis of water-soluble polymer cP1. Reaction conditions: a) bis(pinacolato)diborane, [Pd(dppf)Cl<sub>2</sub>], KOAc, dioxane, 80 °C, 12 h, yield of **1** = 59%; b) 1,6-dibromohexane, K<sub>2</sub>CO<sub>3</sub>, acetone, reflux 48 h, yield of **2** = 60%; c) [Pd(PPh<sub>3</sub>)<sub>4</sub>], K<sub>2</sub>CO<sub>3</sub> (2 M), toluene/H<sub>2</sub>O, 85 °C, 24 h, yield of nP1 = 86%; d) THF/H<sub>2</sub>O, NMe<sub>3</sub>, yield of cP1 = 95%.

and bis(pinacolato)diborane in the presence of KOAc and dioxane at 80 °C for 12 h. The boronic ester was purified by chromatography with silica, and the molecular structure was confirmed by mass spectrometry and NMR spectroscopy. 1,4-Dibromo-2,5-bis(6'-bromohexyloxy)benzene was synthesized in 60% yield by heating a mixture of 2,5-dibromohydroquinone and 1,6-dibromohexane in anhydrous acetone under reflux in the presence of potassium carbonate and [18]crown-6 for 48 h. Quaternization of the pendant groups on the backbone by addition of condensed NMe<sub>3</sub> provided the cationic water-soluble polymer (cP1) in nearly quantitative yield. The degree of quaternization was greater than 90%, as calculated from the ratio of the integrated areas of the signals for CH<sub>2</sub>CH<sub>2</sub>X (X = Br, N(CH<sub>3</sub>)<sub>3</sub>) and CH<sub>2</sub>CH<sub>2</sub>N(CH<sub>3</sub>)<sub>3</sub> in the <sup>1</sup>H NMR spectra. The GPC-determined molecular weight of nP1 (*M*<sub>n</sub>) is about 35 000 amu, with a polydispersity index of 1.9 referenced to polystyrene in THF.

Figure 1 shows the absorption and photoluminescence (PL) spectra of nP1 in THF and cP1 in an aqueous buffer (25 mM sodium phosphate, pH 7.4) and in a 50:50 (v/v) so-

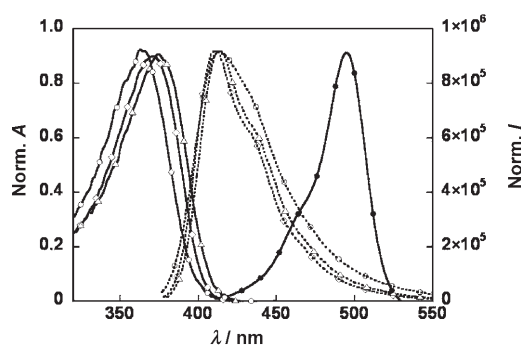


Figure 1. Normalized absorption (solid line) and PL (dashed line) spectra of nP1 in THF (diamonds) and cP1 ([RU] = 1 × 10<sup>-6</sup> M) in aqueous buffer (open circles) and in 50:50 (v/v) THF/buffer (triangles). The absorption of fluorescein is shown by the solid line with filled circles.

lution in THF/buffer. The spectral overlap between the emission of cP1 and the absorption of Fl in buffer is slightly larger than that in THF/buffer. In THF, nP1 displays an absorption maximum ( $\lambda_{\text{abs}}$ ) at 370 nm and a PL maximum ( $\lambda_{\text{PL}}$ ) at 410 nm. In buffer, at a concentration of 1 × 10<sup>-6</sup> M (in polymer repeat units, RUs), the absorption of cP1 underwent a blue shift ( $\lambda_{\text{abs}}$  = 363 nm) relative to that of nP1 in THF, and the PL spectrum slightly broadened, with  $\lambda_{\text{PL}}$  ≈ 415 nm. The spectrum of cP1 in the THF/buffer mixture is slightly narrower than that in buffer alone and more closely resembles that of nP1 in THF.

The changes in the optical properties for cP1 in buffer with varying amounts of THF are shown in Figure 2. The corresponding PL spectra are shown in the Supporting Information. Addition of THF resulted in a slight red shift in the emission maximum. The quantum yield ( $\Phi$ ) of cP1 first increased gradually upon THF addition, then decreased when the THF content was higher than 60%. The  $\Phi$  value of cP1 in buffer is (45 ± 5)%,<sup>[7]</sup> and the highest value, (62 ±

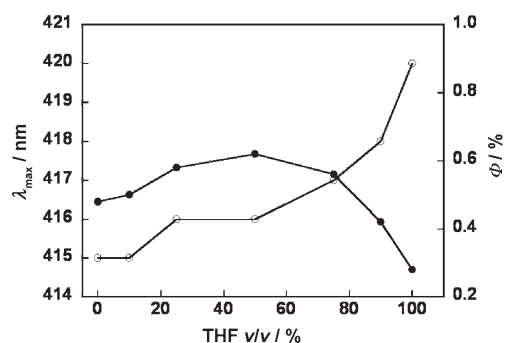


Figure 2. Fluorescence quantum yields (filled circles) and emission maxima (open circles) of cP1 as a function of THF content in buffer (25 mM phosphate buffer, pH 7.4).

5) %, was observed with a 50:50 (v/v) THF/buffer ratio. In the following studies, the 50:50 (v/v) THF/buffer mixture was used. Compared to previous studies, in which a three-fold increase in emission intensity was observed for a cationic poly(fluorene) upon THF addition, the perturbation of THF on the optical properties of cP1 is less pronounced.<sup>[8]</sup>

Direct measurement of oxidation and reduction potentials of cP1 in water was not successful. The HOMO energy level of cP1 was estimated from the oxidation potential of nP1, and the energy of the corresponding LUMO level was obtained by taking into consideration the optical bandgap from the absorption spectra.<sup>[9]</sup> The oxidation potential onset for nP1 is 1.05 V versus a standard calomel electrode (SCE). By taking into account the optical bandgap of 2.85 eV, the nP1 HOMO and LUMO energies were found to be  $-5.45$  and  $-2.6$  eV, respectively.<sup>[10]</sup> The HOMO and LUMO energy levels of nP1 are higher than those of FI ( $-5.9$  and  $-3.6$  eV), thus electron transfer from the former to the latter is energetically favorable.<sup>[5]</sup>

The FRET efficiency upon excitation of cP1 to ssDNA-FI (5'-FI-ATC TTG ACT ATG TGG GTG CT-3') acceptor was examined in buffer in the absence and presence of THF. Measurements were made at a fixed ssDNA-FI concentration ( $2 \times 10^{-8}$  M) and over a range of polymer concentrations ( $[\text{RU}] = 0\text{--}6 \times 10^{-7}$  M). Figure 3a shows the FI emission from cP1/ssDNA-FI in buffer and THF/buffer upon excitation of cP1 ( $[\text{RU}] = 6 \times 10^{-7}$  M) at 363 nm. These spectra show considerably more intense FI emission in the THF/buffer mixture.

PL spectra were also collected upon direct excitation at 490 nm in the absence and presence of cP1 ( $[\text{RU}] = 6 \times 10^{-7}$  M) to examine changes in the intrinsic FI emission. The results are shown in Figure 3b. Compared to direct excitation of FI in the absence of cP1, an 80 % decrease in fluorescence intensity was observed for cP1/ssDNA-FI in THF/buffer. The FI emission was further quenched upon cP1/ssDNA-FI complexation in buffer, to the point that it was difficult to detect by a standard fluorometer. Importantly, similar emission intensities ( $\Phi \approx 0.9$ )<sup>[11]</sup> were observed for ssDNA-FI in both solvents in the absence of cP1. Thus, the changes in the FI emission intensity are likely to be associat-

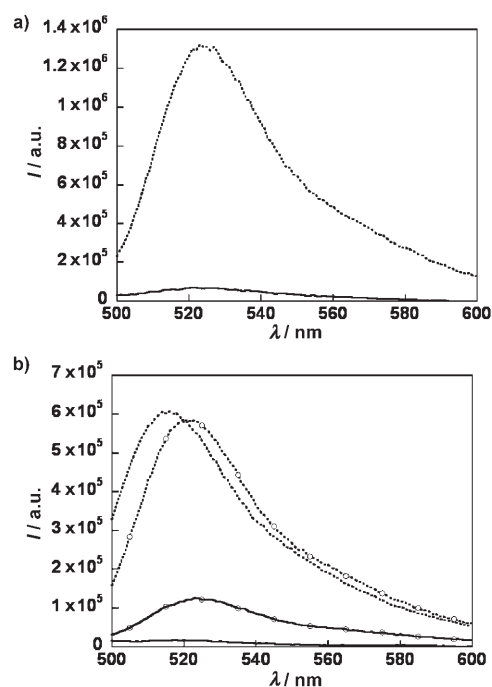


Figure 3. a) PL spectra of ssDNA-FI in the presence of cP1 in THF/buffer (dashed line) and buffer (solid line) upon excitation of cP1 at 363 nm. b) PL spectra of ssDNA-FI in the presence (solid line) and absence (dashed line) of cP1 upon direct FI excitation at 490 nm. Circles = in THF/buffer, no circles = in buffer.

ed with the nature of the cP1/ssDNA-FI complex rather than solvent variations.

Complexation of ssDNA-FI with cP1 led to an increase in the local ssDNA-FI concentration, relative to a homogenous distribution in solution.<sup>[5,12]</sup> This increased concentration can under certain circumstances lead to fluorescence self-quenching.<sup>[5,12]</sup> One way to minimize fluorescence self-quenching without changing the structure of the cP1/ssDNA-FI polyelectrolyte complex substantially is by "diluting" ssDNA-FI with unlabeled ssDNA of an identical nucleotide sequence. We thus monitored the FI emission upon complexation with cP1 in ssDNA-FI/ssDNA mixtures. Measurements were carried out by adding cP1 to solutions that contain  $2 \times 10^{-8}$  M ssDNA-FI in the presence of a total ssDNA concentration of  $1 \times 10^{-6}$  M. Figure 4 provides a comparison of the FI emission in cP1/ssDNA-FI mixtures as a function of solvent and the concentration of cP1.  $F_0$  and  $F$  values correspond to the emission intensities of FI in the absence and presence of cP1, respectively, upon direct FI excitation at 490 nm; the  $F/F_0$  ratio thus provides a measure of fluorescence quenching. Upon direct excitation, the FI emission in THF/buffer was higher than that in buffer regardless of cP1 concentration. At a charge ratio (+/−) of 1.6, at which over 85 % of ssDNA-FI was complexed with cP1 (based on a comparison of the FI emission wavelengths by direct excitation or by FRET from cP1), the higher emission intensity in THF/buffer indicates less quenching of FI emission in the presence of THF, relative to buffer. Importantly, a larger amount of cP1 was required to reach maximum FI

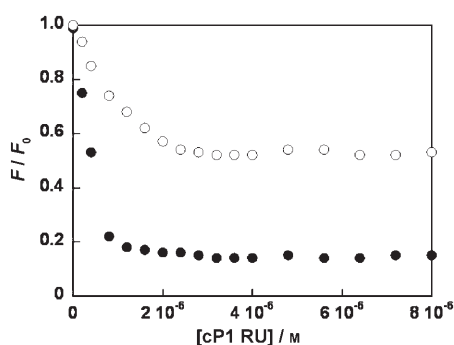


Figure 4. Plot of  $F/F_0$  versus cP1 concentration for cP1/ssDNA-FI + ssDNA mixtures with a total ssDNA concentration of  $1 \times 10^{-6}$  M, prepared by adding cP1 to ssDNA-FI + ssDNA in buffer (filled circles) and THF/buffer (open circles). The excitation wavelength was 490 nm.

quenching in THF/buffer, relative to buffer. This latter observation suggests that the association between ssDNA-FI and cP1 is weaker in the presence of THF, which could result in an increased donor–acceptor distance.

FRET studies of cP1 and ssDNA-FI with the FI “diluted” within the total DNA content ( $[\text{ssDNA-FI}] = 2 \times 10^{-8}$  M,  $[\text{ssDNA}] = 9.8 \times 10^{-7}$  M) are shown in Figure 5. Under these

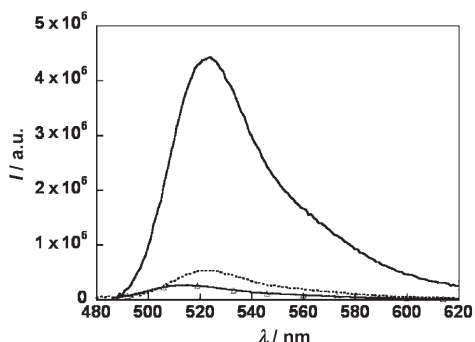


Figure 5. PL spectra of ssDNA-FI in the presence of cP1 in THF/buffer (solid line) and buffer (dashed line) upon excitation of cP1 at 363 nm. The PL spectrum upon excitation of FI at 490 nm in the absence of cP1 is also shown by the solid line with triangles.

conditions, fluorescence self-quenching was minimized. A 20-fold enhancement of the FI emission intensity was observed with a cP1 concentration of  $2 \times 10^{-6}$  M in the presence of THF, relative to direct excitation in the absence of cP1. Similarly, a twofold signal amplification was also observed in buffer. When the results in Figure 5 are compared with those in Figure 3a at the same ssDNA-FI concentration, the net effect of dilution is thus an approximately 10-fold increase in FI emission intensity (upon excitation of cP1), which highlights the contribution of fluorescence self-quenching on signal amplification. All in all, FI emission upon energy transfer in THF with probe dilution is over 100-fold more intense than that obtained in buffer with the same concentration of ssDNA-FI without dilution with ssDNA.

The average lifetime of cP1 in the presence of ssDNA-FI in THF/buffer was calculated to be  $(40 \pm 5)$  ps, which is longer than that measured in buffer.<sup>[13]</sup> This timescale is near the detection limits of our instrument. The reorientation time required for biomolecules of similar size as the cP1/ssDNA-FI complexes was reported to be in the range of several nanoseconds.<sup>[4,14]</sup> Notably, as the lifetime of the excited state of cP1 is much shorter than the motion of the complex, it is unlikely that rotational diffusion of the complex in different solvents could lead to changes in the average orientation factor ( $\kappa$ ). On the other hand, FI is attached to the end of the ss-DNA through a flexible linker, which can spin and wag up and down freely in the solvent. Owing to the randomly formed donor–acceptor pairs in solution, it is unlikely that any changes in orientation for cP1/ssDNA-FI in different solvents could cause such a tremendous difference in the sensing of FI emission.

The fluorescence decay of acceptor FI (cP1/ssDNA-FI) in buffer and THF/buffer was monitored upon excitation of cP1 with 390-nm laser pulses. Experiments were conducted at ssDNA-FI and cP1 concentrations of  $1 \times 10^{-7}$  and  $5 \times 10^{-7}$  M, respectively. Direct excitation of FI at 390 nm did not result in measurable emission; thus, any measured emission in cP1/ssDNA-FI solutions is a result of energy transfer. The fluorescence lifetime at 520 nm of ssDNA-FI in THF/buffer was measured to be 3.8 ns, which is very close to the values reported for FI attached to protein and ss-DNA (3.8–4.5 ns).<sup>[15]</sup> For cP1/ssDNA-FI in buffer, the lifetime of FI decreased to 3.0 ns. This change in lifetime indicates possible electron transfer between the polymer and FI, and the tendency towards more-rapid fluorescence decay in more-polar solvents agrees well with the previous report.<sup>[16]</sup> Efforts made to capture the charge-separated species by using transient absorption were not successful, primarily because of the low concentrations of the complexes. Obvious precipitation was observed at high concentrations. The higher FI emission upon energy transfer in THF/buffer thus mostly reflects the reduced electron transfer.

The FRET efficiency upon excitation of cP1 to dsDNA-FI (5'-FI-ATC TTG ACT ATG TGG GTG CT-3' hybridized with its complementary sequence 5'-AGC ACC CAC ATA GTC AAG AT) was also examined in buffer in the absence and presence of THF. FRET measurements were carried out at a fixed dsDNA-FI concentration ( $2 \times 10^{-8}$  M) and over a range of polymer concentrations ( $[\text{RU}] = 0\text{--}6 \times 10^{-7}$  M). Figure 6 compares the FI emission from cP1/dsDNA-FI in buffer and THF/buffer upon excitation of cP1 at 363 nm upon addition of cP1. Under these experimental conditions, much stronger FI emission was observed in the THF/buffer mixture. Notably, in buffer, maximum FI emission occurred at a charge ratio (+/−) slightly greater than 1, whereas a larger amount of cP1 (+/− > 2) was required to reach maximum FI emission. The latter observation indicates weaker cP1/ssDNA association in the presence of THF.

The effect of THF on DNA-duplex stability was studied by monitoring the absorption of dsDNA-FI ( $1 \times 10^{-6}$  M) at 260 nm in buffer and in buffer/THF (50:50 v/v) as a function



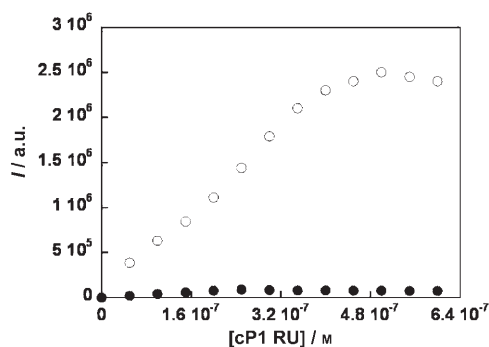


Figure 6. Integrated emission intensity of FI for cP1/dsDNA-FI in THF/buffer (open circles) and buffer (filled circles) as a function of cP1 concentration. The excitation wavelength was 363 nm.

of temperature. It was found that the melting profile of dsDNA in THF/buffer was shifted to lower temperatures relative to that in buffer (see Supporting Information). Melting temperatures were calculated to be 50°C (THF/buffer) and 58°C (buffer); they were determined by taking the maximum of the first derivative of a melting transition measured by the absorption. Both melting curves share similar shapes, indicating that the DNA molecules were in duplex format and the organic solvent did not alter the DNA conformation significantly at room temperature. Similar observations have been reported previously in a study of the effect of organic solvents on dsDNA conformation.<sup>[17]</sup>

## Conclusions

In summary, self-quenching and photoinduced electron transfer together are major mechanisms for the low FI emission upon excitation of cP1 in buffer. The improved sensitization of fluorescence by cP1 observed by addition of THF is probably due to an increase in the FI emission yields. We have identified two effects that may be responsible for these observations. First, it is well-established that reducing solvent polarity decreases the driving force for electron transfer.<sup>[18]</sup> By adding THF to the aqueous buffer (50:50 v/v), we obtained a solvent mixture with a dielectric constant ( $\epsilon$ ) of about 40 at room temperature,<sup>[19]</sup> which is considerably lower than that of the buffer ( $\epsilon=80$ ). Electron transfer should thus be disfavored. Second, the association between cP1 and ssDNA-FI is weaker, as determined by the less-pronounced decrease in  $F/F_0$  as a function of cP1 concentration prior to  $F/F_0$  saturation (Figure 4). Less cP1 is needed in buffer than in THF/buffer to reach maximum quenching. The weaker binding between cP1 and ssDNA-FI in THF/buffer may also lead to conditions whereby electron transfer is reduced by virtue of the larger separation between optically active units and the more-acute dependence of electron-transfer efficiency on donor-acceptor distance, relative to FRET.<sup>[20]</sup> Despite mechanistic uncertainties, the sensitivities of CCP-based sensors that operate by energy transfer to FI-labeled bimolecular probes may be considerably im-

proved by the addition of small portions of suitable organic solvents.

## Experimental Section

### General Details

$^1\text{H}$  and  $^{13}\text{C}$  NMR spectra were recorded on Varian ASM-100 200 MHz spectrometers. UV/Vis absorption spectra were recorded on a Shimadzu UV-2401 PC diode array spectrometer. Fluorescence was measured by using a PTI (Lawrenceville, NJ) Quantum Master fluorometer equipped with a xenon-lamp excitation source and a Hamamatsu (Japan) 928 photomultiplier tube, with 90° angle detection for solution samples. Reagents were obtained from Aldrich Co. and were used as received.

Quantum yields were measured by using quinine sulfate as the standard, with a quantum yield of 54.6% in  $\text{H}_2\text{SO}_4$  (0.1 N). Cyclic voltammetry data of nP1 were collected in THF with  $\text{Bu}_4\text{NPF}_6$  (0.1 M) as the electrolyte at a scan rate of 100 mV s<sup>-1</sup>. A glassy carbon electrode (1.6-mm diameter) was used as the working electrode, and Pt wire and Ag/AgNO<sub>3</sub> were used as the auxiliary and reference electrodes, respectively. For measurement of FRET efficiency, all the spectra were corrected against the detector profile to normalize the difference in detector sensitivity at different wavelengths. At each excitation wavelength, the optical gain was automatically adjusted by the instrument to normalize the xenon output at different wavelengths.

### Syntheses

**1,4-Dibromo-2,5-bis(6-bromohexyloxy)benzene:** 2,5-dibromohydroquinone (5.4 g, 20 mmol), potassium carbonate (13.8 g, 0.2 mol), [18]crown-6 (50 mg), and 1,6-dibromohexane (36.5 mL, 0.24 mol) were mixed in 200 mL of anhydrous acetone and heated under reflux for 48 h. After the reaction mixture was cooled to room temperature, acetone and excess 1,6-dibromohexane were removed by vacuum distillation. The residue was extracted with dichloromethane and washed with 5% sodium hydroxide solution followed by water. The organic layer was separated and dried over magnesium sulfate. After removal of the solvent, the crude product was recrystallized with a mixture of chloroform and hexane to afford 1,4-dibromo-2,5-bis(6-bromohexyloxy)benzene (3.6 g, 60%) as white crystals.  $^1\text{H}$  NMR (200 MHz,  $\text{CDCl}_3$ ):  $\delta$  = 7.09 (s, 2H), 3.95 (t, 4H), 3.42 (t, 4H), 1.87–1.82 (m, 8H), 1.55–1.50 ppm (m, 8H);  $^{13}\text{C}$  NMR (50 MHz,  $\text{CDCl}_3$ ):  $\delta$  = 150.0, 118.5, 111.1, 69.9, 33.8, 32.6, 28.9, 27.8, 25.2 ppm.

**Bis[9,9'-bis(6''-bromohexyl)fluorenyl]-4,4,5,5-tetramethyl[1.3.2]dioxaborolane:** 9,9'-Bis(bromohexyl)-2,7-dibromofluorene (6.5 g, 10 mmol), bis(pinacolato)diborane (6.0 g, 24 mmol), KOAc (7.0 g, 70 mmol), and dioxane (100 mL) were mixed together. After degassing,  $[\text{Pd}(\text{dppf})\text{Cl}_2]$  (0.5 g;  $\text{dppf}$  = 1,1'-bis(diphenylphosphanyl)ferrocene) was added. The reaction mixture was kept at 85°C overnight, then cooled to room temperature. The organic solvent was distilled out, and the residual solid was dissolved in dichloromethane and washed with water. After drying with  $\text{Na}_2\text{SO}_4$ , the solvent was distilled out. The crude product was purified by flash chromatography (hexanes/dichloromethane = 2:1) to give a white solid (4.2 g, 59%).  $^1\text{H}$  NMR (400 MHz,  $\text{CDCl}_3$ ):  $\delta$  = 7.83–7.72 (m, 6H), 3.25 (t,  $J$  = 6.8 Hz, 4H), 2.03–1.99 (m,  $J$  = 4.0 Hz, 4H), 1.64–1.57 (m,  $J$  = 7.2 Hz, 4H), 1.39 (s, 24H), 1.17–1.13 (m, 4H), 1.06–1.02 (m, 4H), 0.58–0.53 ppm (m, 4H);  $^{13}\text{C}$  NMR (100 MHz,  $\text{CDCl}_3$ ):  $\delta$  = 150.3, 144.1, 134.0, 128.9, 119.7, 84.0, 55.2, 40.1, 34.2, 32.8, 29.2, 27.9, 23.6 ppm; MS (EI):  $m/z$  = 744 [ $M$ ]<sup>+</sup>.

**nP1:** 2,7-Bis[9,9'-bis(6''-bromohexyl)fluorenyl]-4,4,5,5-tetramethyl[1.3.2]dioxaborolane (372 mg, 0.5 mmol), 1,4-dibromo-2,5-bis(6-bromohexyloxy)benzene (297 mg, 0.5 mmol),  $[\text{Pd}(\text{PPh}_3)_4]$  (5 mg), tetrabutylammonium bromide (40 mg), and potassium carbonate (828 mg, 6 mmol) were placed in a 25-mL round-bottomed flask. A mixture of water (3 mL) and toluene (5 mL) was added to the flask, and the reaction vessel was degassed. The mixture was vigorously stirred at 85°C for 24 h and then precipitated into methanol. The polymer was filtered and washed with methanol and acetone, then dried under vacuum for 24 h to afford nP1.

(399 mg, 86 %) as white fibers.  $^1\text{H}$  NMR (200 MHz,  $\text{CDCl}_3$ ):  $\delta$  = 7.85–7.57 (m, 6H), 7.13 (s, 2H), 4.01 (t, 4H), 3.35 (t, 4H), 3.29 (t, 4H), 2.0–0.8 ppm (m, 36H);  $^{13}\text{C}$  NMR (50 MHz,  $\text{CDCl}_3$ ):  $\delta$  = 150.4, 150.1, 139.9, 137.1, 131.3, 128.1, 124.4, 119.5, 116.9, 69.6, 54.9, 40.5, 33.9, 33.8, 32.7, 29.3, 27.8, 23.9 ppm.

cP1: Condensed trimethylamine (2 mL) was added dropwise to a solution of nP1 (50 mg) in THF (10 mL) at  $-78^\circ\text{C}$ . The mixture was allowed to warm to room temperature. The precipitate was redissolved by the addition of water (10 mL). After the mixture was cooled to  $-78^\circ\text{C}$ , more trimethylamine (2 mL) was added, and the mixture was stirred for 24 h at room temperature. After removal of the solvent, acetone was added to precipitate cP1 (55 mg, 95 %) as a white powder.  $^1\text{H}$  NMR (200 MHz,  $\text{CD}_3\text{OD}$ ):  $\delta$  = 7.91–7.67 (m, 6H), 7.20 (s, 2H), 4.13 (br, 4H), 3.40 (br, 8H), 3.18 (s, 18H), 3.10 (s, 18H), 2.0–0.8 ppm (m, 36H);  $^{13}\text{C}$  NMR (50 MHz,  $\text{CD}_3\text{OD}$ ):  $\delta$  = 152.0, 151.6, 141.5, 138.9, 132.6, 129.8, 125.6, 120.7, 117.7, 70.8, 67.8, 50.4, 30.6, 25.2, 24.2, 24.0 ppm.

The double-stranded DNA (5'-Fl-ATC TTG ACT ATG TGG GTG CT-3' together with its complementary sequence 5'-AGC ACC CAC ATA GTC AAG AT) was obtained by annealing mixtures of the complementary strands in phosphate buffer solution (50 mM) at  $70^\circ\text{C}$  for 20 min and then slowly cooling to room temperature. Melting curves of dsDNA-Fl were monitored in both phosphate buffer (25 mM) as well as in buffer/THF mixtures, from 20 to  $75^\circ\text{C}$  (buffer) or from 20 to  $65^\circ\text{C}$  (THF/buffer) with increments of  $1^\circ\text{Cmin}^{-1}$ . Melting temperatures were determined from the corresponding melting curves.

## Acknowledgements

We thank the National University of Singapore (NUS ARF R-279-000-197-112 and R-279-000-197-133), the National Institutes of Health (GM 62958-01), and the NSF (DMR-0097611) for financial support. We also thank Prof. Qinghua Xu from the Chemistry Department of the National University of Singapore for measurements of lifetime and valuable discussion.

- [1] a) L. H. Chen, D. W. McBranch, H. L. Wang, R. Helgeson, F. Wudl, D. G. Whitten, *Proc. Natl. Acad. Sci. USA* **1999**, *96*, 12287–12292; b) D. T. McQuade, A. E. Pullen, T. M. Swager, *Chem. Rev.* **2000**, *100*, 2537–2574; c) K. P. R. Nilsson, O. Inganäs, *Nat. Mater.* **2003**, *2*, 419–424; d) B. Liu, G. C. Bazan, *Chem. Mater.* **2004**, *16*, 4467–4476; e) M. D. Disney, J. Zheng, T. M. Swager, P. H. Seeberger, *J. Am. Chem. Soc.* **2004**, *126*, 13343–13346; f) M. R. Pinto, K. S. Schanze, *Proc. Natl. Acad. Sci. USA* **2004**, *101*, 7505–7510; g) J. H. Wosnick, C. M. Mello, T. M. Swager, *J. Am. Chem. Soc.* **2005**, *127*, 3400–3405; h) M. Leclerc, H. A. Ho, *Synlett* **2004**, *2*, 380–387; i) H. A. Ho, M. Leclerc, *J. Am. Chem. Soc.* **2004**, *126*, 1384; j) F. Le Floch, H. A. Ho, L. P. Harding, M. Bedard, P. R. Neagu, M. Leclerc, *Adv. Mater.* **2005**, *17*, 1251–1254; k) N. DiCesare, R. Pinto, K. S. Schanze, J. R. Lakowicz, *Langmuir* **2002**, *18*, 7785–7787; l) D. T. McQuade, A. H. Hegedus, T. M. Swager, *J. Am. Chem. Soc.* **2000**, *122*, 12389–12390; m) K. P. R. Nilsson, A. Herland, P. Hammarström, O. Inganäs, *Biochemistry* **2005**, *44*, 3718–3724.
- [2] a) B. S. Gaylord, A. J. Heeger, G. C. Bazan, *Proc. Natl. Acad. Sci. USA* **2002**, *99*, 10954–10957; b) S. Wang, G. C. Bazan, *Adv. Mater.* **2003**, *15*, 1425–1428; c) B. Liu, G. C. Bazan, *J. Am. Chem. Soc.* **2004**, *126*, 1942–1943; d) B. S. Gaylord, A. J. Heeger, G. C. Bazan, *J. Am. Chem. Soc.* **2003**, *125*, 896–900; e) B. Liu, S. Baudrey, L. Jaeger, G. C. Bazan, *J. Am. Chem. Soc.* **2004**, *126*, 4076–4077; f) B. Liu, S. Wang, G. C. Bazan, A. Mikhailovsky, *J. Am. Chem. Soc.* **2003**, *125*, 13306–13307.
- [3] T. Förster, *Ann. Phys.* **1948**, *2*, 55–75.
- [4] J. R. Lakowicz, *Principles of Fluorescence Spectroscopy*, Kluwer Academic/Plenum Publishers, New York, **1999**.
- [5] B. Liu, G. C. Bazan, *J. Am. Chem. Soc.* **2006**, *128*, 1188–1196.
- [6] D. M. Guldi, A. Swartz, C. P. Luo, R. Gómez, J. Segura, N. Martín, *J. Am. Chem. Soc.* **2002**, *124*, 10875–10886.
- [7] J. N. Demas, G. A. Crosby, *J. Phys. Chem.* **1971**, *75*, 991–1024.
- [8] S. Wang, G. C. Bazan, *Chem. Commun.* **2004**, 2508–2509.
- [9] R. Gomer, G. Tryson, *J. Chem. Phys.* **1977**, *66*, 4413–4424.
- [10] A. J. Bard, L. R. Faulkner, *Electrochemical Methods*, John Wiley & Sons, New York, **1980**.
- [11] With fluorescein in 0.1 M NaOH (pH 11) as a reference, with a quantum yield of 92 %.
- [12] a) E. Van Rompaey, N. Sanders, S. C. De Smedt, J. Demeester, E. Van Craenenbroeck, Y. Engelborghs, *Macromolecules* **2000**, *33*, 8280–8288; b) B. Lucas, K. Remaut, K. Braeckmans, J. Hastraete, S. C. De Smedt, J. Demeester, *Macromolecules* **2004**, *37*, 3832–3840.
- [13] The lifetime was measured by using a time-correlated single-photon-counting technique.
- [14] L. J. Parkhurst, K. M. Parkhurst, R. Powell, J. Wu, S. Williams, *Biopolymers* **2002**, *61*, 180.
- [15] a) A. K. Tong, S. Jockusch, Z. M. Li, H. R. Zhu, D. L. Akins, N. J. Turro, J. Y. Ju, *J. Am. Chem. Soc.* **2001**, *123*, 12923–12924; b) “Data Table—1.5 Fluorescein, Oregon Green and Rhodamine Green Dyes”, to be found under <http://probes.invitrogen.com/servlets/datatable?id=32077>, **2006**; c) H. Elmgren, *J. Polym. Sci. Polym. Lett. Ed.* **1980**, *18*, 815–822.
- [16] K. R. J. Thomas, A. L. Thompson, A. V. Sivakumar, C. J. Bardeen, S. Thayumanavan, *J. Am. Chem. Soc.* **2005**, *127*, 373–383.
- [17] G. Löber, H. Schütz, *Biopolymers* **1972**, *11*, 2439–2459.
- [18] C. Lambert, J. Schelter, T. Fiebig, D. Mark, A. Trifonov, *J. Am. Chem. Soc.* **2005**, *127*, 10600–10610.
- [19] F. E. Critchfield, J. A. Gibson, J. L. Hall, *J. Am. Chem. Soc.* **1953**, *75*, 6044–6045.
- [20] a) J. N. Clifford, E. Palomares, M. K. Nazeeruddin, M. Grätzel, J. Nelson, X. Li, N. J. Long, J. R. Durrant, *J. Am. Chem. Soc.* **2004**, *126*, 5225–5233; b) M. W. Wu, *Phys. Lett. A* **1997**, *230*, 237–243.

Received: August 7, 2006

Revised: January 16, 2007